Assessment of FY3A and FY3B/MWHS observations

Keyi Chen[1,2,3], Stephen English[4] and Jiang Zhu[1]

[1] International Center for Climate and Environment Sciences, Institute of Atmospheric Physics, China.

[2] University of Chinese Academy of Sciences.

[3] The Department of Atmospheric Sciences, Chengdu University of Information & Technology.

[4] European Centre for Medium-Range Weather Forecasts

Summary

The FY3 series began in May 2008 with the launch of the FY-3A satellite. The microwave humidity sounders (MWHS) provide vertical information of water vapour, which is important for numerical weather prediction (NWP). The Noise Equivalent Delta Temperature (NEDT) of the MWHS is higher than that of the Microwave Humidity Sounder instrument (e.g. on MetOp-B) but lower than that on the older AMSU-B instruments (on NOAA-15, 16 and 17). Assimilation of MWHS observations into the ECMWF Integrated Forecast System (IFS) improved the fit of short range forecasts to other observations, notably MHS and also slightly improved the longer range forecast scores verified against analysis. Also assimilating both the MWHS/FY3A and the MWHS/FY3B gave a larger impact than either instrument alone. However some negative impacts were also found. These forecast errors appeared to originate in the Tropics and spread southwards. This may imply an improved quality control (QC) is needed in the tropics. These encouraging results suggest that the FY3 series MWHS data is close to the quality required for use in NWP assimilation systems.

1. Introduction

China launched the first FY3 satellite in May 2008. This was the second generation of the Chinese polar orbiting satellites, carrying significantly more sophisticated sensors for operational meteorology than the first generation. The first two satellites in the series, FY-3A and FY-3B, were classed as research satellites. In September 2013, the third satellite (FY-3C) was launched as the first operational satellite. The microwave instruments onboard have the potential to play an important role in Numerical Weather Prediction (NWP). Therefore, a detailed assessment of the data quality of these microwave radiometers on the preparatory FY3 satellites is required.

Since the FY-3 series are expected to become an important data source for NWP, reanalysis and climate sciences, this assessment has already begun. Lu et al. (2011) assessed the microwave temperature sounder (MWTS) against a baseline of the operational ECMWF NWP short range forecast, using the RTTOV radiative transfer model (Saunders et al 1999). Significant biases were found and it was suggested that this were related to both to shifts in the frequency of the channel pass-bands and radiometer non-linearity. After these effects were properly accounted for the data quality of MWTS and MWHS was found to be broadly comparable with AMSU-A and MHS in terms of its global bias of NWP simulations (Zou .et.al. 2011). Observing system experiments suggested that the impacts were neutral to slightly positive, which was very encouraging and built confidence that the following series of the FY3 instruments would be widely used in NWP data assimilation systems (Lu et al. 2011). The studies to date focused primarily on the MWTS. In this study the focus is on the humidity sounder, the MWHS.

In section 2, the microwave humidity sounders from FY3 series and MetOp-B are described and compared; section 3 presents the data quality assessment based on statistical analysis of the first-guess departures; the data assimilation experiments by the ECMWF operational modeling are described in section 4 and some conclusions are drawn in section 5.

2. Microwave Humidity Sounders

2.1 *MWHS data*

The FY3 series MWHS is a five-channel cross-track scanning instrument able to provide vertical humidity information to the NWP data assimilation systems. The vertical resolution is poor, with only 2 to 3 pieces of independent information. Nonetheless this has been proven valuable to NWP in the past. The central frequencies of MWHS are shown in the Table 1. It measures microwave radiation at five channels 150GHz (V), 150GHz (H), 183.31±1GHz (V), 183.31±3GHz (V) and 183.31±7GHz (V). The nominal spatial resolution is 15km at nadir and the swath width is 2700km with a total of 98 FOVs (field of view) along each scan-line (Table 2).

Channel number		Frequency (GHz)		Bandwidth (MHz)	
MHS	MWHS	MHS	MWHS	MHS	MWHS
1	1	89(V)	150(V)	1400×2	1000×2
2	2	157(V)	150(H)	1400×2	1000×2
3	3	183.31±1(H)	183.31±1(V)	500×2	500×2
4	4	183.31±3(H)	183.31±3(V)	1000×2	1000×2
5	5	190.31(V)	183.31± (V)	1000×2	1100×2

Table 1. MHS and MWHS channels characteristics

2.2 *MHS data*

The MHS used in this report is onboard the MetOp-B satellite and is also a cross-track scanning microwave radiometer. It also has five channels, but with slightly different frequencies to the MWHS: 89GHz (surface), 157GHz (H), 183.31±1GHz (V), 183.31±3GHz (V) and 190.31 (V). The nominal spatial resolution is the same with MWHS at nadir, but the swath width is smaller than MWHS, only 2250KM, with a total of 90 FOVs along each scan-line (Table 2). This means that in the tropics MWHS has smaller gaps between consecutive orbits than MHS.

Channel number		Nadir Res. (km)		WF (hPa)		Swath width (km)	
MHS	MWHS	MHS	MWHS	MHS	MWHS	MHS	MWHS
1	1	15	15	surface	surface	2250	2700
2	2	15	15	surface	surface	2250	2700
3	3	15	15	400	400	2250	2700
4	4	15	15	600	600	2250	2700
5	5	15	15	800	800	2250	2700

Table 2. MHS and MWHS channels characteristics

3. **Data quality assessment**

Figure 1 compares the MWHS and the corresponding MHS channel 3 fit to the ECMWF short range forecast and analysis. In these plots the statistics for all data is plotted (i.e. including data that does not pass quality control checks). The standard deviation of the first-guess departure (O-B) of the MWHS is larger with larger variations with time than that of the MHS (Fig1 (a)-(b)). The number of MWHS observations available also varies more than is found for MHS (Fig1 (c)-(d)).

In order to decrease the geophysical noise, a clear dataset was defined based on a criterion that the first-guess departures of channel 1 is below 5K. The clear data of MWHS is compared with the MHS that passes quality control tests for assimilation in the ECMWF forecasting system, which is called used data. Also since the emissivity of the land is more complex, the data is compared only over sea (Figure 2). A spike occurred on 10th July in the time series of

the standard deviation of the first-guess departure (O-B) of the MWHS, while no such kind of spike appears in the MHS used data.

This spike clearly relates to an anomaly in the MWHS data. The first-guess departures with the absolute value larger than 15K on the spike day (July 10th, 2013) are plotted in Figure 3 and show that this is occurred for a small number of scan lines, suggesting an error in the calibration. However with the data available it is not possible to diagnose why the calibration was wrong for these scan lines.

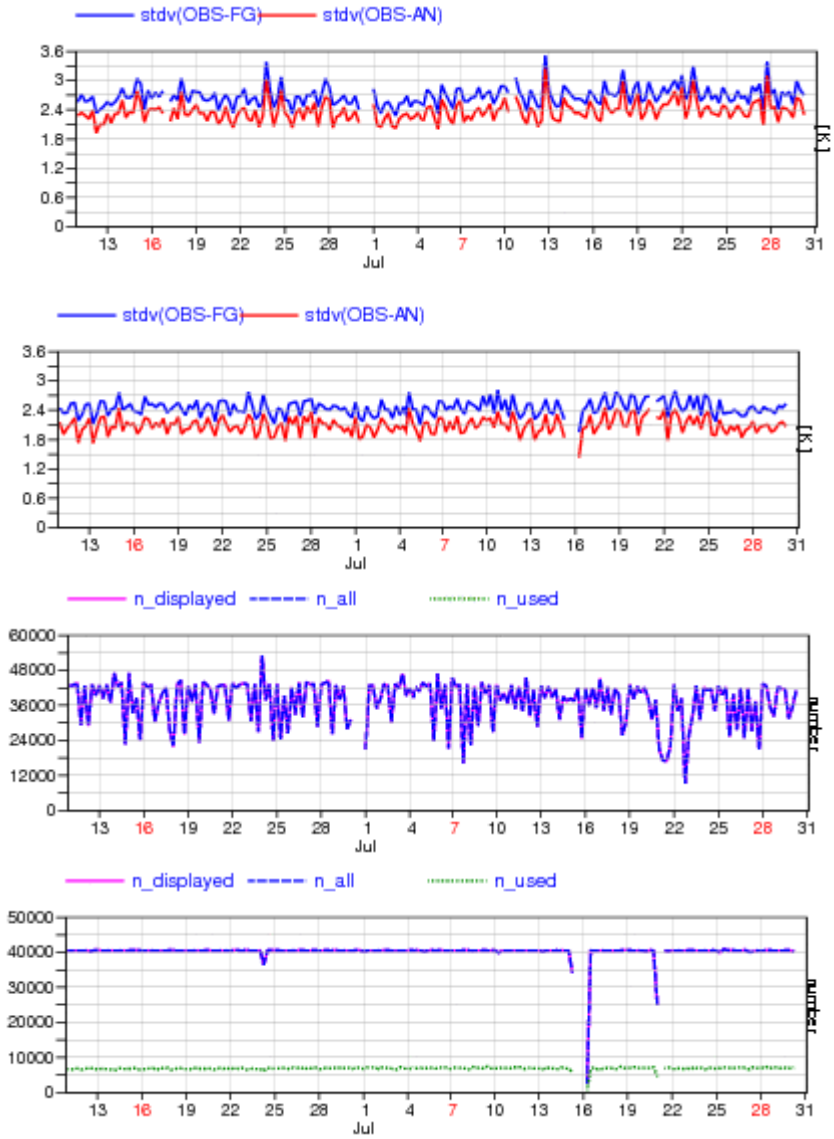

Figure 1. (a) the time series of the standard deviation of the first-guess departure (O-B) of the MWHS channel 3 for all data; (b) the time series of the standard deviation of the first-guess departure (O-B) of MHS channel 3 for all data; (c) the time series of the 6-hourly sample number of the MWHS; (d) the time series of the 6-hourly sample number of MHS.

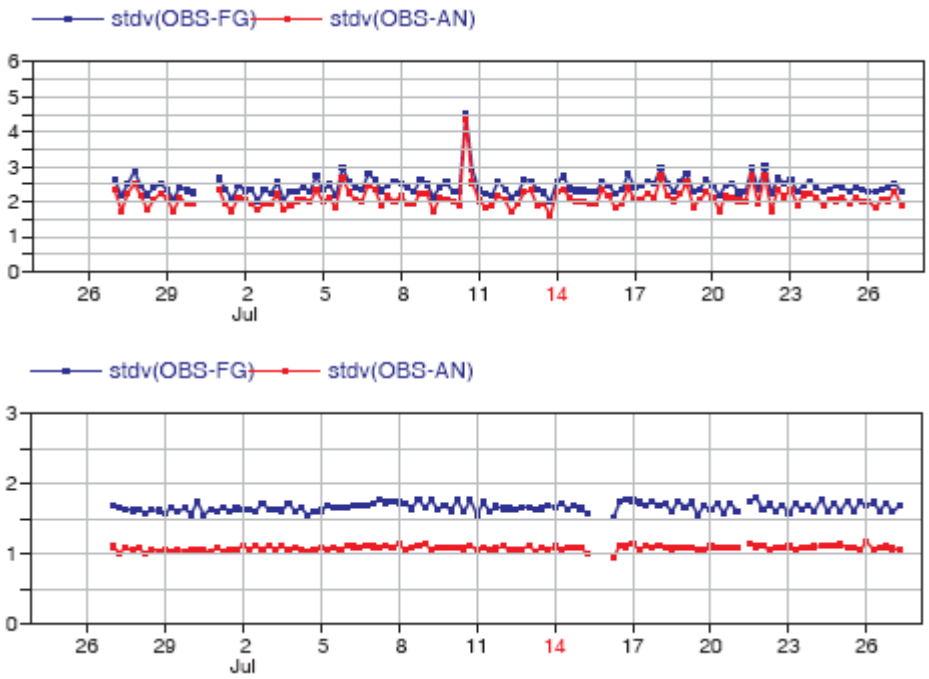

Figure 2. (a) the time series of the standard deviation of the first-guess departure (O-B) of the MWHS channel 3 for clear data over sea; (b) the time series of the standard deviation of the first-guess departure (O-B) of MHS channel 3 for used data over sea.

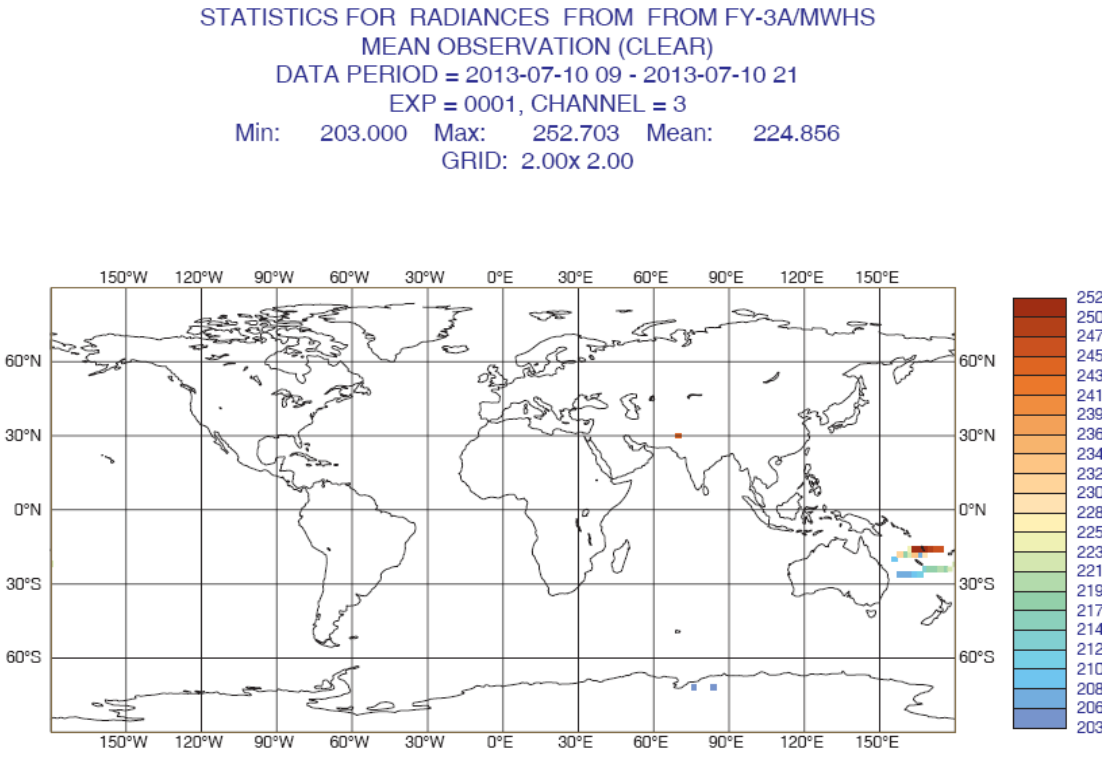

Figure 3. Locations of the first-guess departures with the absolute value larger than 15K on July 10th, 2013.

4. Data Assimilation Experiments

4.1 Experiment Set up

As the monitoring showed that, in general, MWHS data is of good quality the MWHS data has been experimentally assimilated into the ECMWF forecasting system (IFS) and its

impacts are analyzed. To minimize the influence from the data noise and the complex surface emissivity, only the clear data over sea is used and all the data over land, sea ice or with wrong geographic information is excluded.

Three experiments are run to test the impacts from the MWHS assimilation. The control run has no MWHS assimilated and assimilation of other observations matches the ECMWF operational system on these dates. The control (Exp ID is fz1w) was run from the July 10th, 2013 to the September 10th, 2013 and forecast times are 00Z and 12Z each day, which provide 125 forecast samples in total. The experiments used ECMWF cycle 38R2 with a T511 spectral truncation, corresponding to a spatial resolution of around 40km The first experiment added the MWHS on FY3A a(ID fz1u).. The second experiment added the MWHS on FY3B with the experiment period from the July 7th, 2013 to the September 7th, 2013. The IDs are fz1y and fz1z for control and experiment respectively. The third experiment (Exp ID is fzc0) added both the MWHS/FY3A and MWHS/FY3B into the assimilation system at the same time with the same experiment period.

4.2 Assimilation output

After assimilation, the probability density function of the first-guess departure of MWHS and MHS are compared (Figure 4). The MWHS data (blue line) has higher noise than MHS (red line). To quantify this, artificial noise is added to each channel of MHS (only channel 3 figures are shown.). The two curves are very similar after 0.3K of random noise is added.

Figure 5 indicates that the quality control (QC) employed in the IFS removes the badly calibrated scan lines identified in section 3. The time series of MWHS is much smoother than that in figure 2, but because MWHS has more noise, the value of the standard deviation of the first-guess departure and its variation with time are still larger than MHS. It is very interesting to notice that after assimilation, the MWHS 6-hour sample number varies like a wave-shape with time, while the MHS sample number does not. This is due to the assimilation priority of MHS, therefore, if MWHS data has the overlap in space and time with MHS data, only MHS is used to eliminate data redundancy. The date (00Z, August 10th, 2013) with the least MWHS used sample is picked out and sample distributions of MWHS and MHS are displayed by figure 6. Obviously, the missing sample of MWHS overlapped with MHS in space and time and the MWHS sample number variation period with time depends on the time difference between MWHS and MHS.

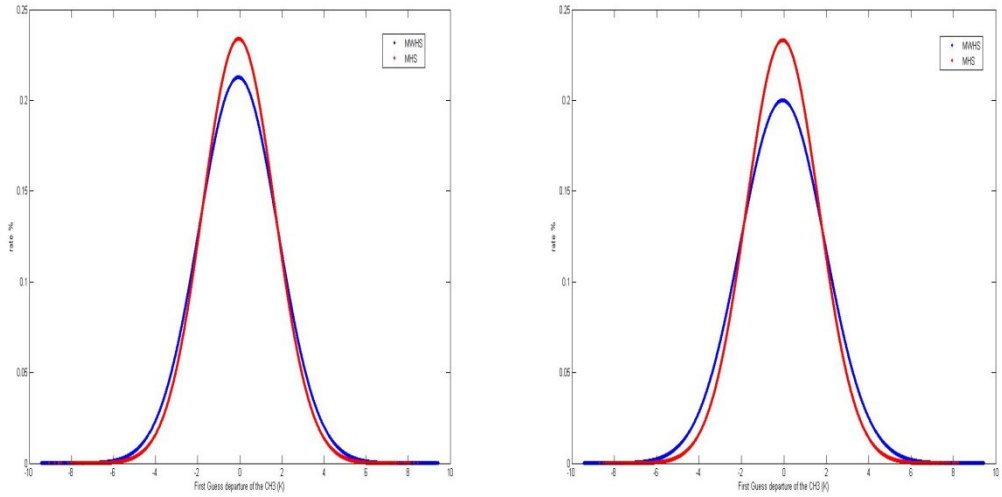

(a) (b)

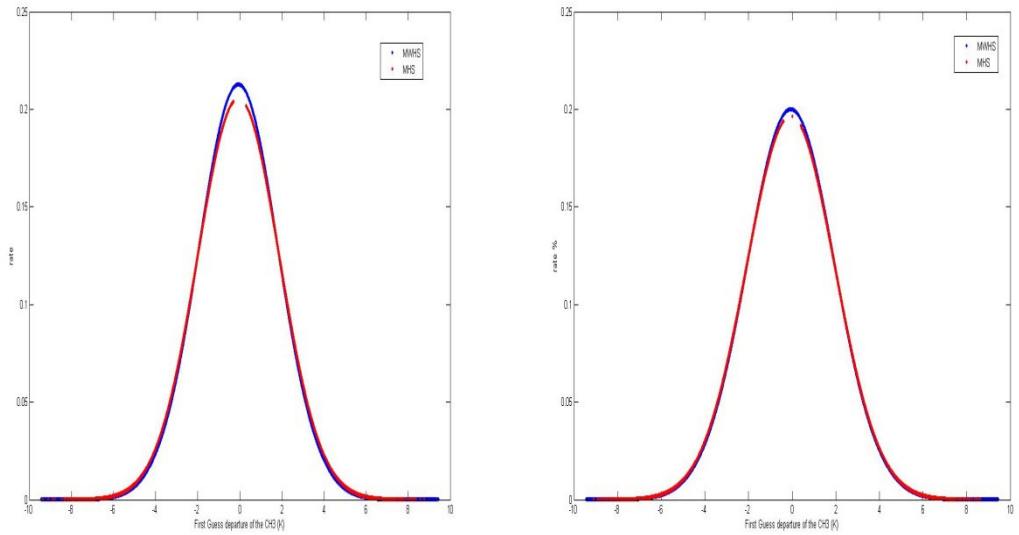

(c) (d)

Figure 4. The probability density functions of the first-guess departure of MWHS and MHS. MWHS/FY3A .vs. MHS; (b) MWHS/FY3B .vs. MHS; (c) MWHS/FY3A .vs. MHS with noise 0.3K added; (d) MWHS/FY3B .vs. MHS with noise 0.3K added.

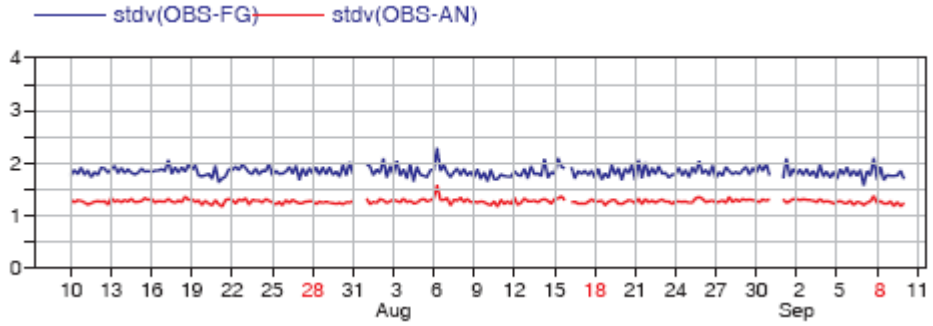

(a)

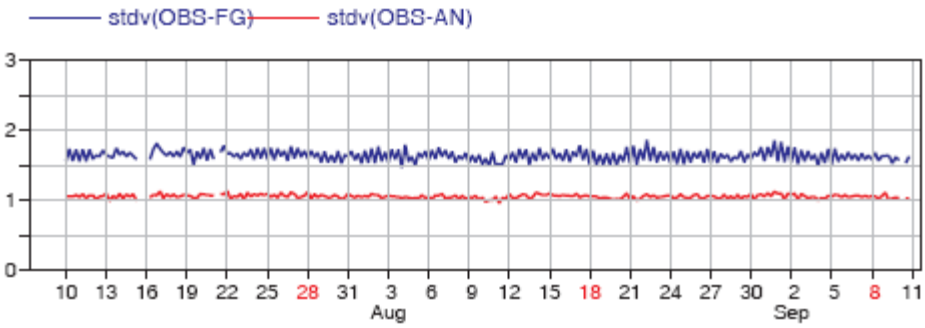

(b)

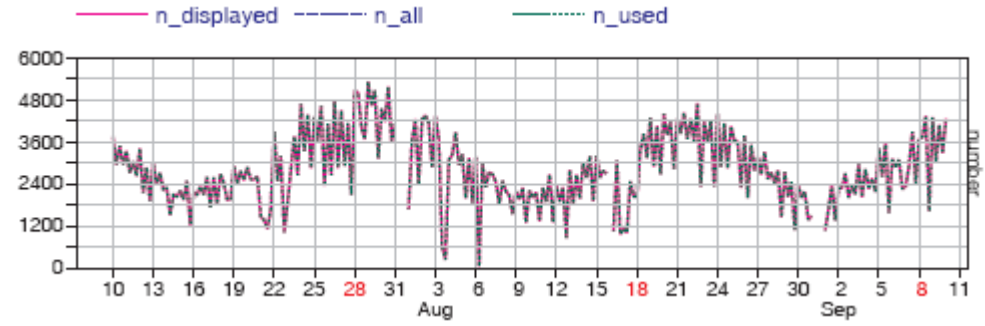

(c)

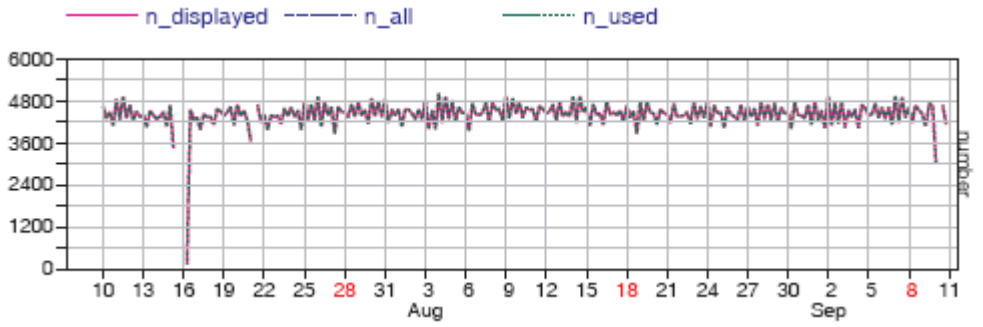

(d)

Figure 5. (a) the time series of the standard deviation of the first-guess departure (O-B) of the MWHS in channel 3 for used data over sea; (b) the time series of the standard deviation of the first-guess departure (O-B) of the MHS in channel 3 for used data over sea; (c) the time series of the 6-hourly sample number of the MWHS used data; (d) the time series of the 6-hourly sample number of MHS used data.

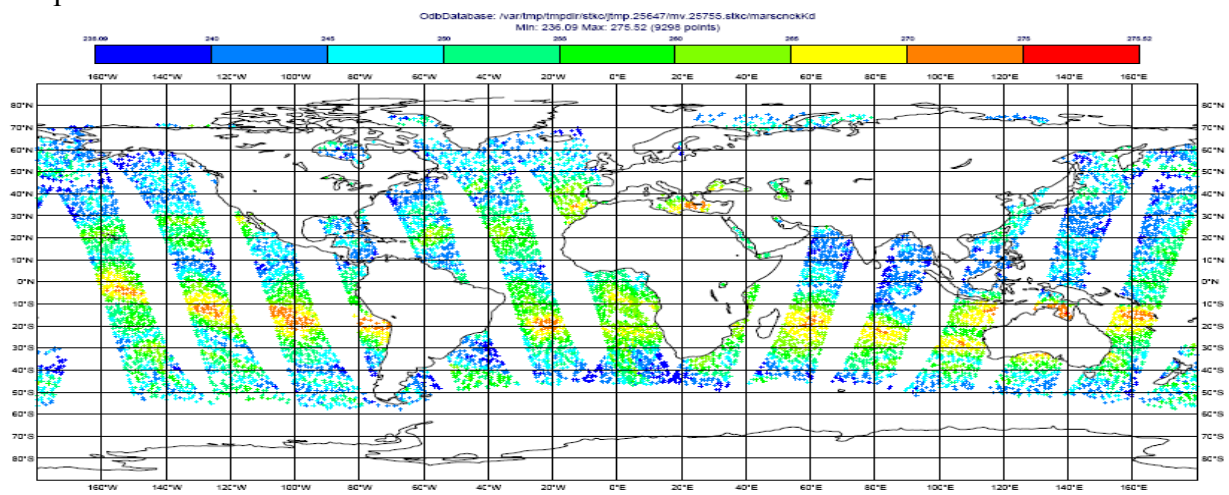

(a)

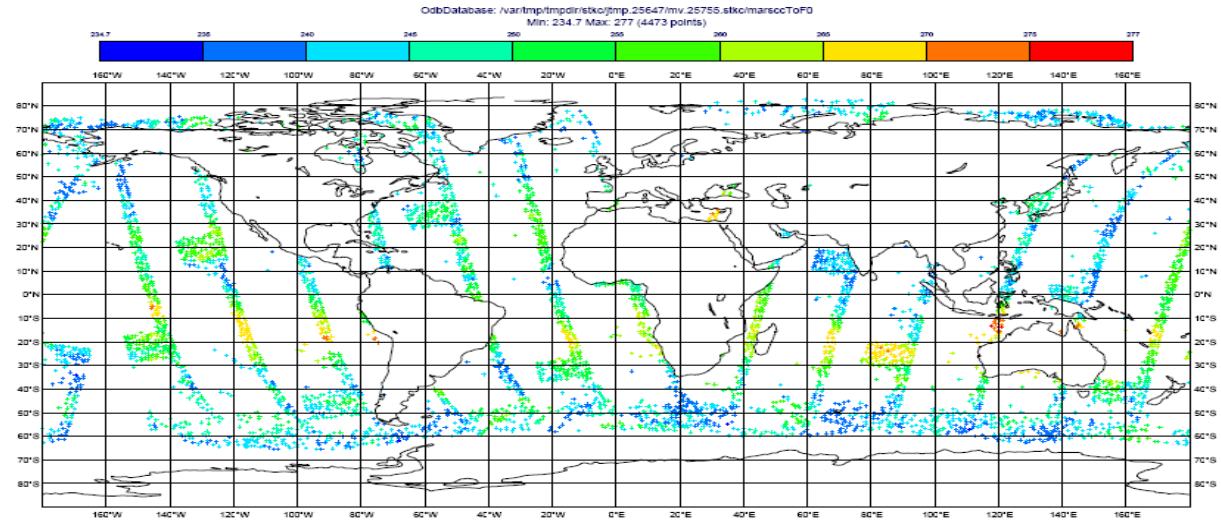

(b)

Figure 6. The 6-hour sample distributions at 00Z, August 10th, 2013; (a) of MHS, (b) of MWHS.

The assimilation output shows that after the FY3 series MWHS data put into the ECMWF system, it does not degrade the whole assimilation system (figures are not shown.). Globally, it decreases the standard deviation of the first-guess and analysis departures (O-B) of MHS. Similar improvements were found in North Hemisphere, South Hemisphere and Tropics, respectively (not shown). Even better results come out from assimilation with MWHS/FY3A and MWHS/FY3B together (Figure 7). The black line is for the combination of both MWHS instruments and the red line is for the FY3A or FY3B instrument individually. The standard deviations of the first-guess departure (O-B) and analysis departure of MHS are reduced more with the combination of both instruments than when only one is used.

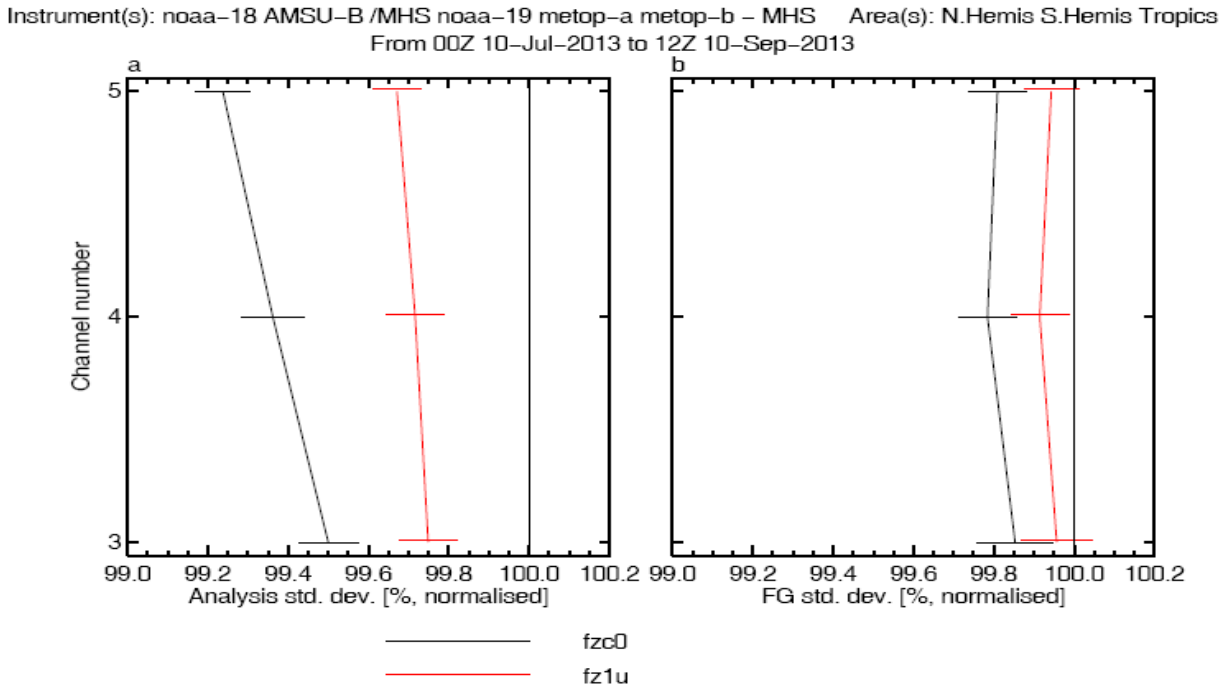

(a)

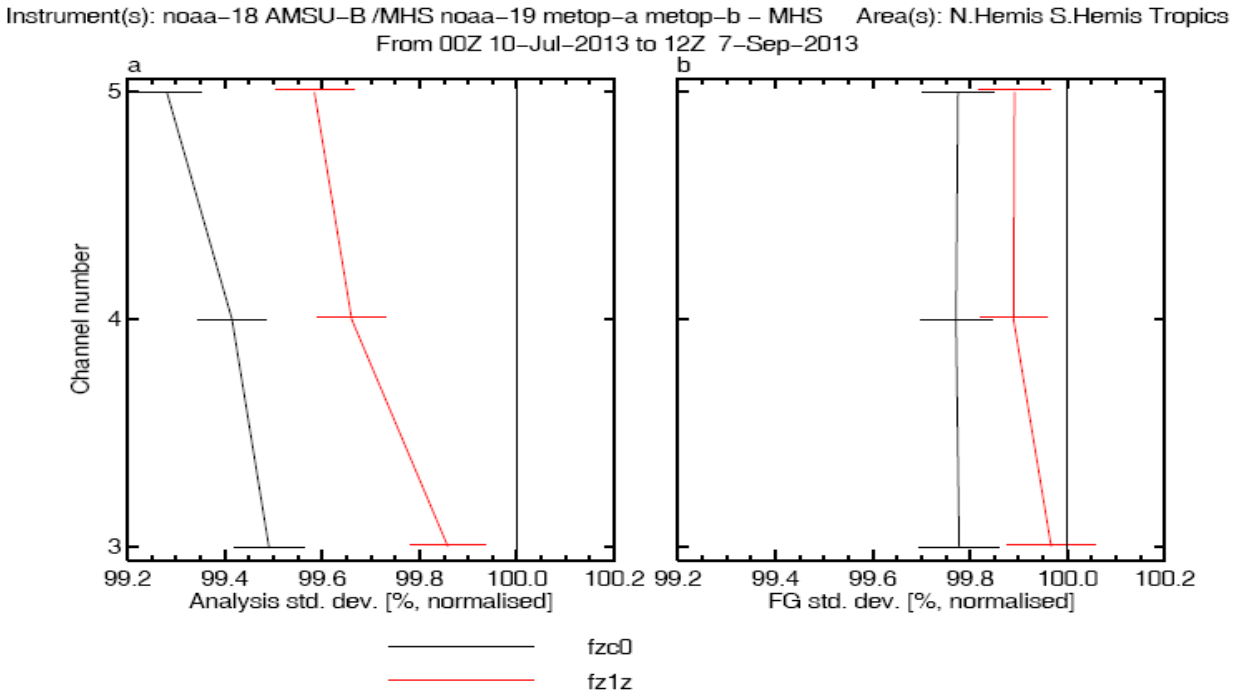

(b)

Figure 7. The normalised standard deviation of the first-guess departures and the analysis departures of MHS after assimilation with (a) FY3 series combination .vs. FY3A/MWHS and (b) FY3 series combination .vs. FY3B/MWHS input.

4.3 Forecast Assessment

The impacts of the assimilation with MWHS on FY3 on the forecast have been evaluated. The forecast scores show positive results in the North Hemisphere , and are found to be neutral in the South Hemisphere and Tropics (Figures are not shown.). The scores are verified against both the ECMWF operational analysis and observations with similar results. The forecast error change at a range of forecast range, latitude and altitude is shown bin Figure 8. Only the plots of the vector wind are shown here, as this is one of the key forecast variables known to have sensitivity to humidity assimilation in 4D-var. Positive impacts are displayed in blue. Forecast errors are decreased more in the North Hemisphere when both MWHSs are assimilated. In the South Hemisphere and the Tropics, both decreased forecast errors and increased forecast errors are seen. It is noticed that the increased forecast errors are very significant around the region of 30° South. This degradation is more noticeable for FY3B than FY3A.

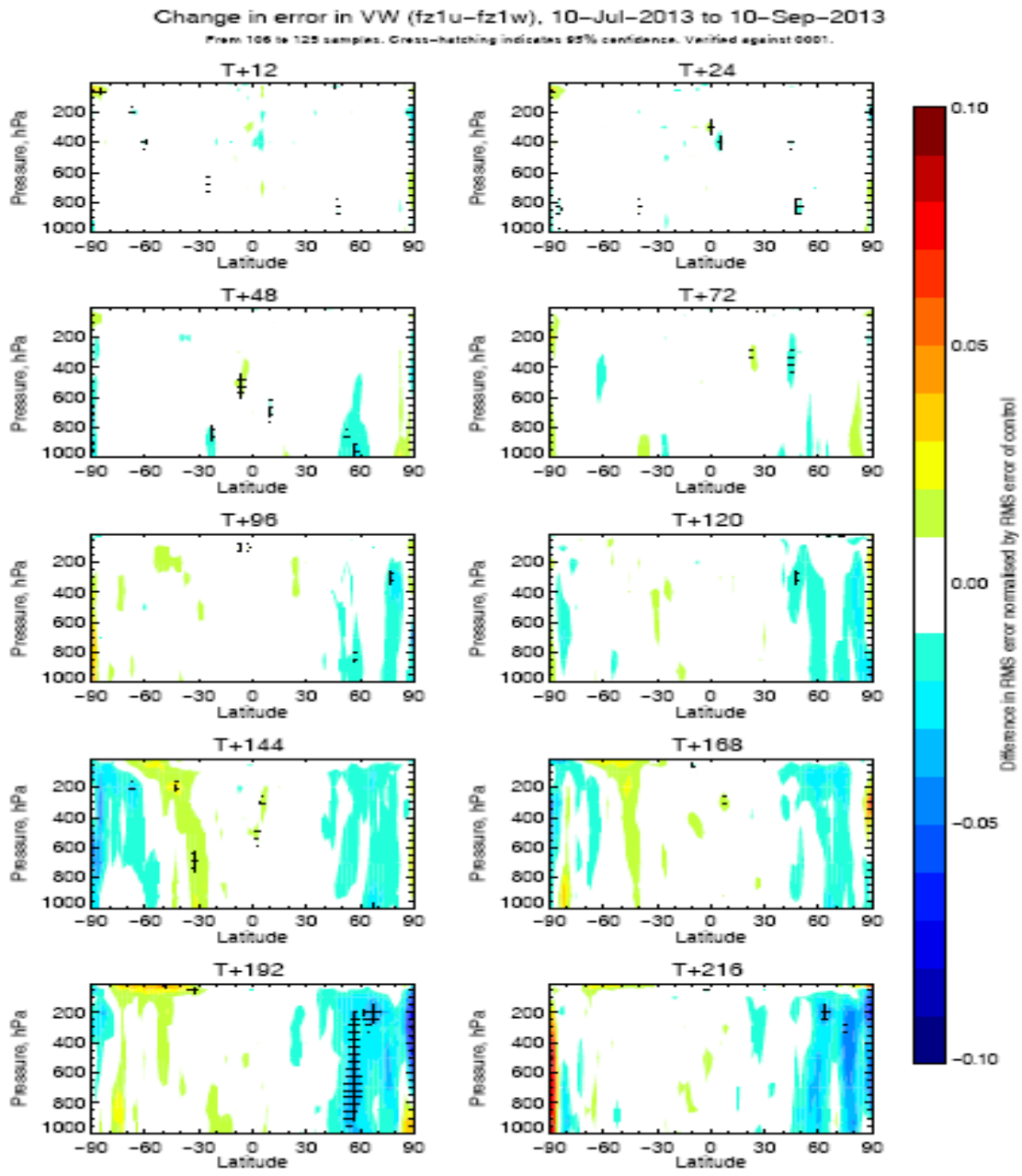
Change in error in VW (fz1u–fz1w), 10–Jul–2013 to 10–Sep–2013
From 106 to 125 samples. Cross–hatching indicates 95% confidence. Verified against 0001.
T+12
T+24
T+48
T+72
T+96
T+120
T+144
T+168
T+192
T+216
Pressure, hPa
Latitude
Difference in RMS error normalised by RMS error of control
0.10
0.05
0.00
−0.05
−0.10

(a)

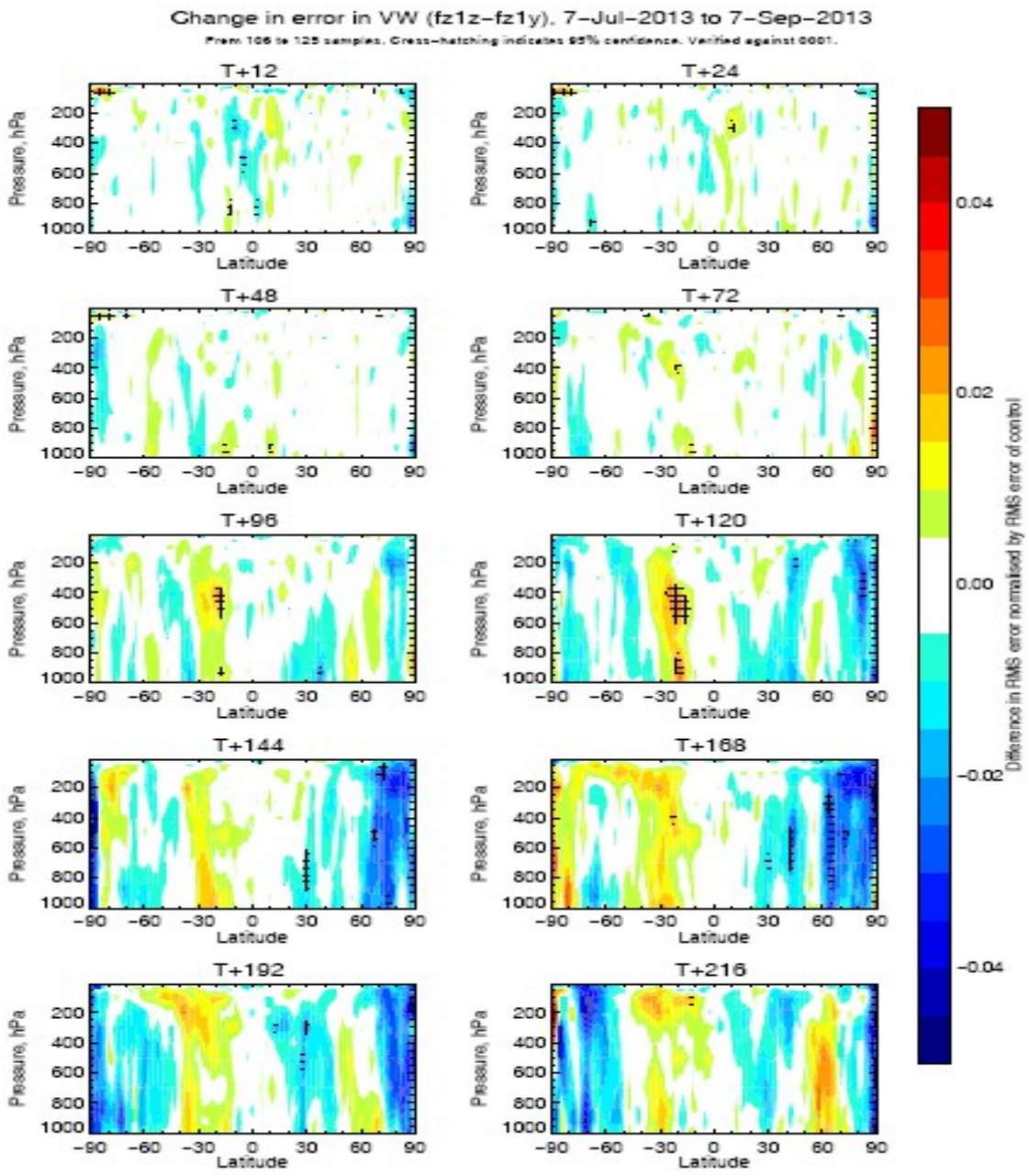
Change in error in VW (fz1z−fz1y), 7−Jul−2013 to 7−Sep−2013
From 106 to 125 samples. Cross−hatching indicates 95% confidence. Verified against 0001.
T+12
T+24
T+48
T+72
T+96
T+120
T+144
T+168
T+192
T+216
Pressure, hPa
Latitude
Difference in RMS error normalised by RMS error of control
0.04
0.02
0.00
−0.02
−0.04

(b)

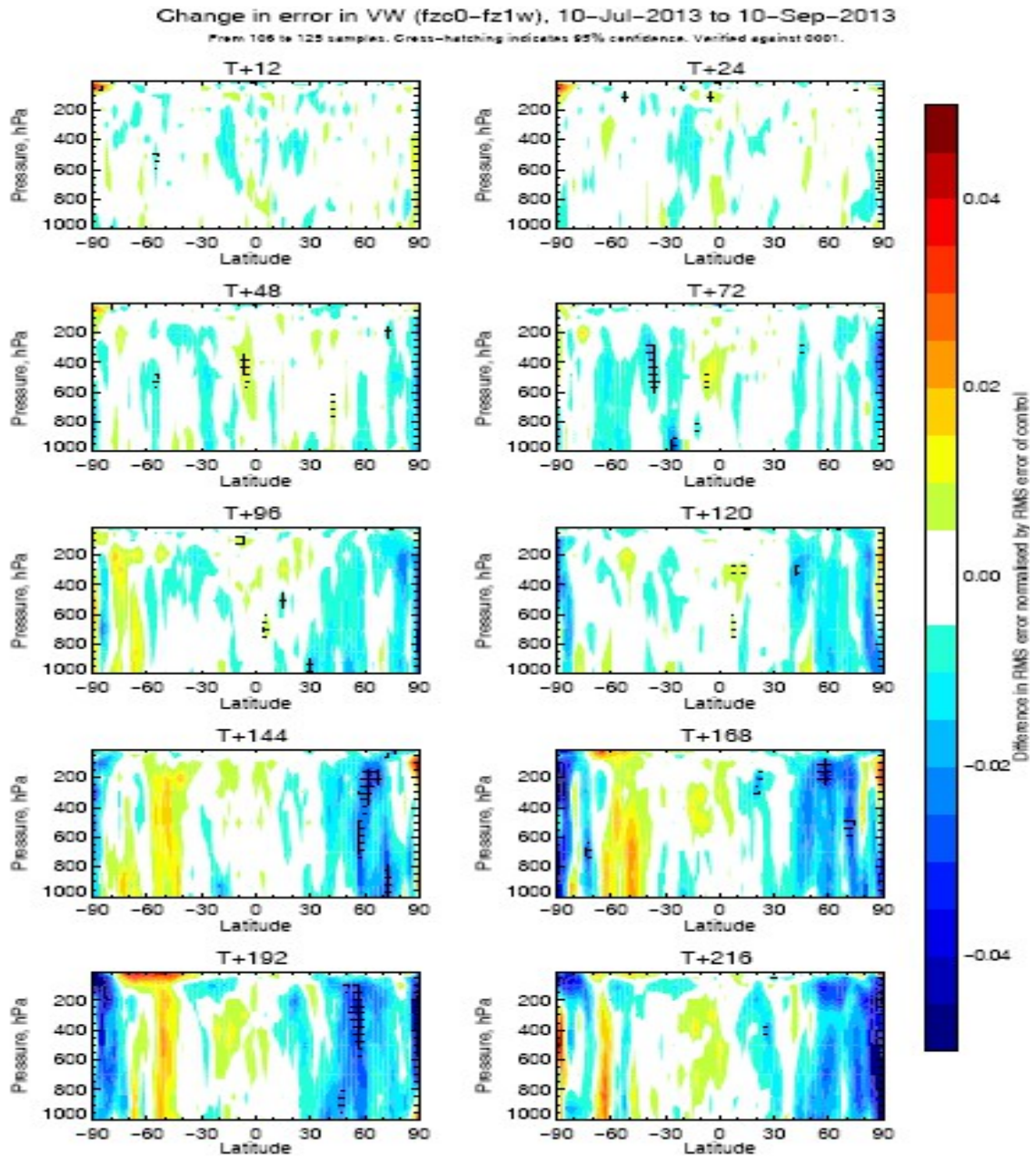

(c)

Figure 8. Cross-sections of the forecast errors of the vector wind with time with (a) MWHS/FY3A assimilated; (b) MWHS/FY3B assimilated; (c) both MWHS/FY3A and MWHS/FY3B assimilated. Cross-hatching indicates 95% confidence. Blue indicates the reduced forecast errors.

Since the increased forecast errors are largest between 600hPa and 400hPa in Figure8 (b), forecast error maps at 500hPa at a range of forecast times are shown in Figure 9. Increased forecast errors are found in the Southern Hemisphere. These errors can be traced back to analysis changes in the Tropics. Therefore, the forecast errors start from the Tropics, mainly spread southward, and grow stronger with time. In order to reduce the forecast errors, tighter quality control (QC) may well be needed in the Tropics and future work will be done to investigate this.

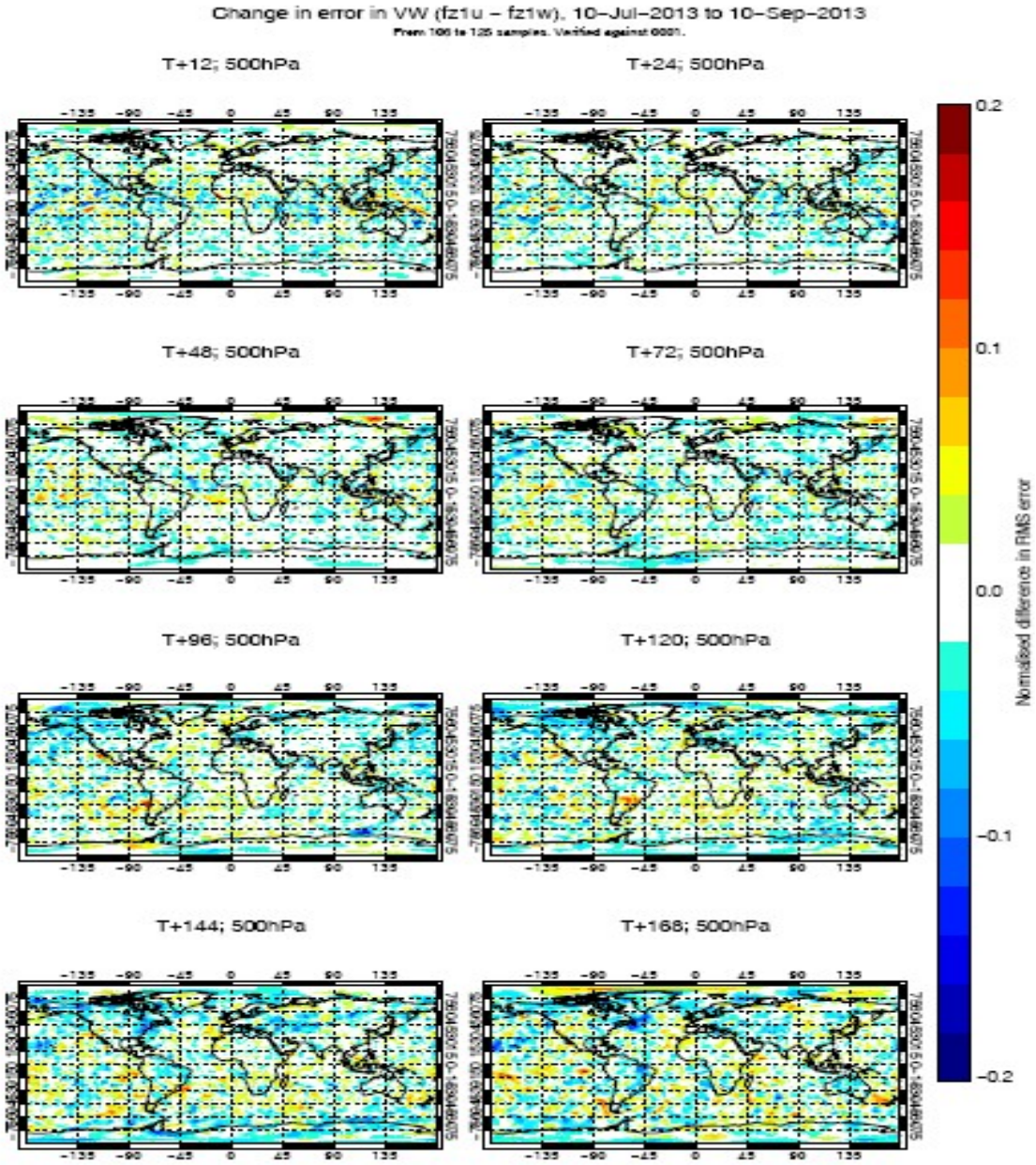
Change in error in VW (fz1u – fz1w), 10–Jul–2013 to 10–Sep–2013
From 106 to 125 samples. Verified against 0001.
T+12; 500hPa
T+24; 500hPa
T+48; 500hPa
T+72; 500hPa
T+96; 500hPa
T+120; 500hPa
T+144; 500hPa
T+168; 500hPa
0.2
0.1
0.0
−0.1
−0.2
Normalised difference in RMS error

(a)

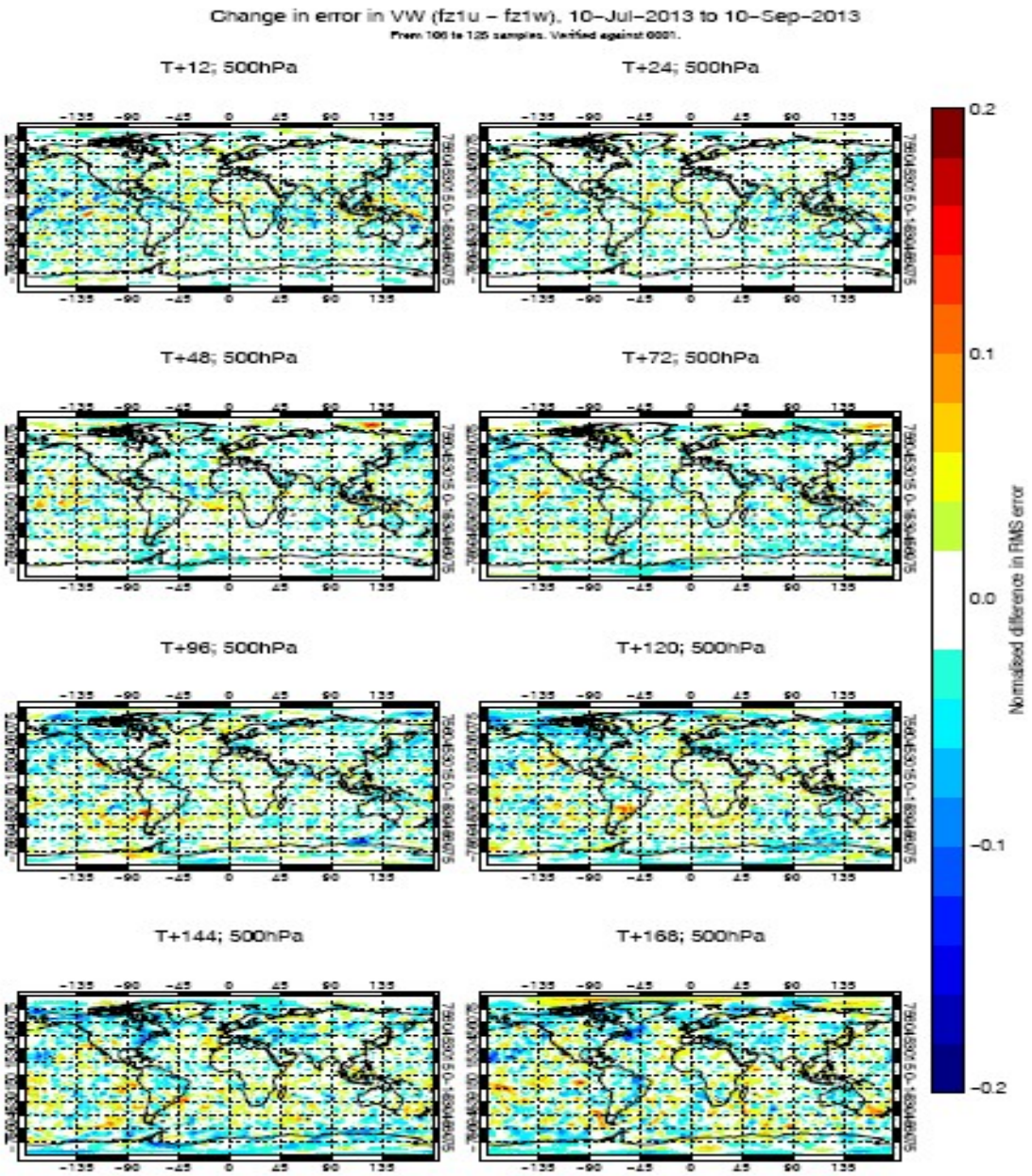
Change in error in VW (fz1u – fz1w), 10–Jul–2013 to 10–Sep–2013
From 100 to 125 samples. Verified against 0001.
T+12; 500hPa
T+24; 500hPa
T+48; 500hPa
T+72; 500hPa
T+96; 500hPa
T+120; 500hPa
T+144; 500hPa
T+168; 500hPa
0.2
0.1
0.0
−0.1
−0.2
Normalised difference in RMS error

(b)

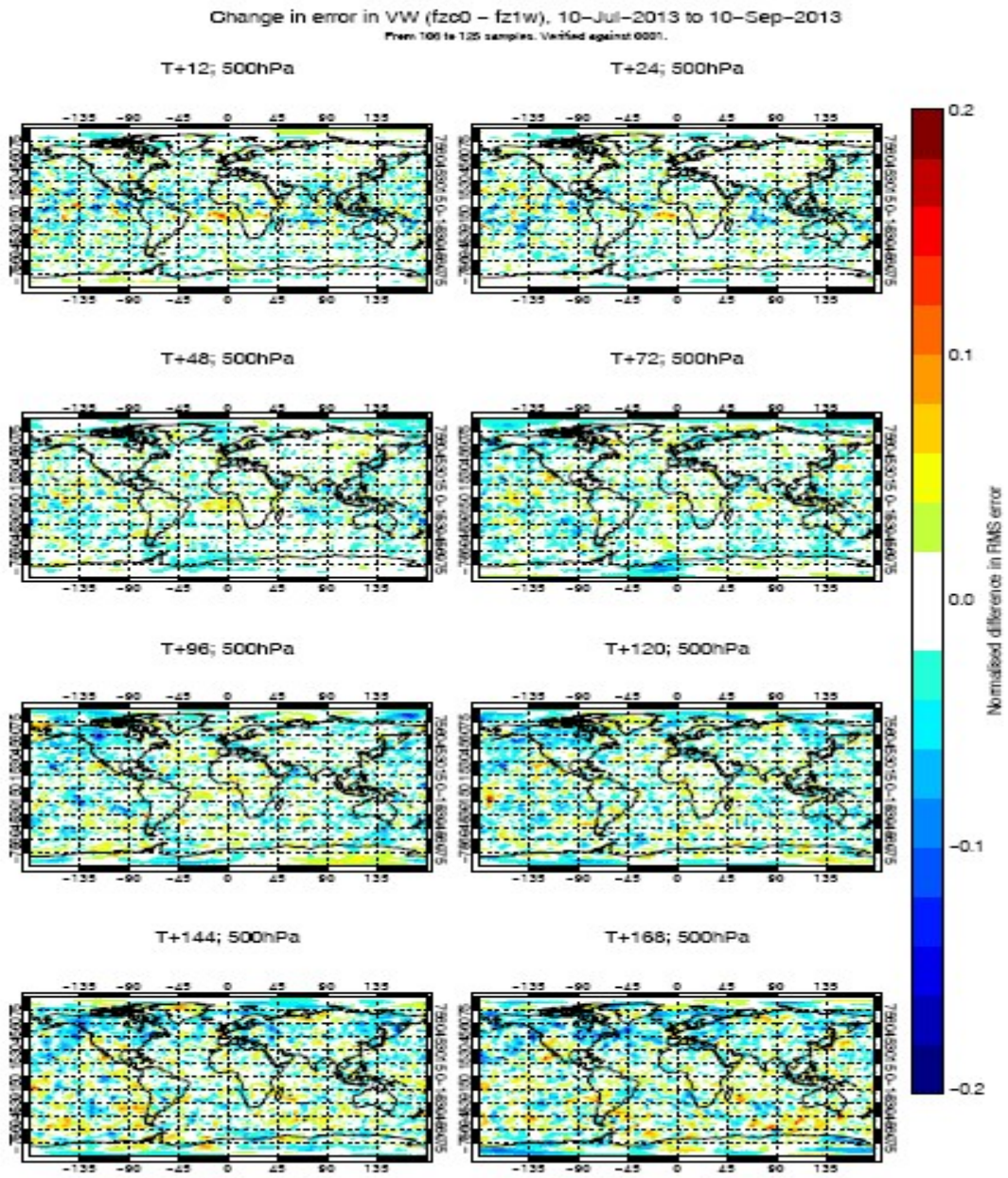

(c)

Figure 9. The vector wind forecast errors distribution maps at 500hPa with time with (a) MWHS/FY3A assimilated; (b) MWHS/FY3B assimilated; (c) both MWHS/FY3A and MWHS/FY3B assimilated. Blue indicates the reduced forecast errors.

5. *Conclusions*

Data from the microwave humidity sounding instruments on the FY3 satellites has been tested in the ECMWF Integrated Forecasting System (IFS). This permits both an assessment of data quality through an analysis of first-guess departures statistics, compared with the equivalent MetOp-B instruments, as well as evaluation of the potential impact on operational forecasts through data assimilation experiments. The first-guess departure statistics indicate that MWHS data has higher noise than MHS data. There are also occasional calibration issues seen in first-guess departures that in the period studied here were removed successfully by quality control, but need to be understood. This demonstrates that more monitoring of the calibration should be done during the ground processing. .

The data quality assessment by the assimilation experiments and operational forecasts provides valuable information on the impacts of the data on numerical weather prediction

analysis and forecast scores. In the experiments presented here, the MWHS instruments were able to indicate neutral to slightly positive impact not only on humidity but also on the forecasts of vector winds. The forecast errors in the North Hemisphere are reduced more than that in the South Hemisphere and the Tropics. Improvements are larger when two MWHSs are assimilated (FY3A and FY3B) than when only one is used. Some increased forecast errors are found to originate from changes in the Tropical analysis. These spread southward and grow stronger with time. Tighter quality control processes (QC) may be needed to avoid this problem before MWHS can be used operationally. Since all the experiments here are run during the Northern Hemisphere summer, the experiments should be repeated in the Northern Hemisphere winter to confirm that differences between the hemispheres are not a summer: winter effect.

The data from the MWHS on the FY3 series has given a promising impact on the NWP forecasting quality. Similar assessment of the microwave radiation imager (MWRI) and the infrared atmospheric sounder (IRAS) is needed.

6. Acknowledgments:

This work is also supported by China's Research and Development Special Fund for Pub-licWelfare Industry (Meteorology GYHY(QX)200906006) by providing part of travel funds.

7. Reference:

Bell, W., and Coauthors, 2008. The assimilation of SSMIS radiances in numerical weather prediction models. IEEE Trans. Geosci. Remote Sens., 46, 884–900.

Durand, Y., Bougeault, P., Pierrard. M. C., 1989. 'Utilisation des mesures satellitaires dans le systkme d'assirnilation *B* mtsoechelle PERIDOT. Premikre partie:I x modkle d'analyse.' Working Note ARPEGE No. 6; available from Direction de la ttkorologie Nationale,Paris

English SJ., Saunders, R., Candy, B., Forsythe, M., Collard, AP., 2004. Met Office Satellite Data Observing System Experiments. In 3rd WMO Workshop on the Impact of Various Observing Systems in NumericalWeather Prediction, Alpbach, Austria.

Eyre, J., 1991. A fast radiative transfer model for satellite sounding systems. ECMWF Technical Memorandum.

Geer, A. J., Bauer, P., Bormann, N., 2010: Solar biases in microwave imager observations assimilated at ECMWF. IEEE Trans. Geosci. Remote Sens., 48, 2660–2669.

Grody, N. C., Vinnikov, K. Y., Goldberg, M. D., Sullivan, J. T., and Tarpley, J. D., 2004. Calibration of multisatellite observations for climatic studies: Microwave Sounding Unit (MSU). J. Geophys. Res., 109, D24104, doi:10.1029/2004JD005079.

Guan, L., Zou, X., Wang, X., Weng, F., Li, G., 2011. Assessments of FY-3A Microwave Humidity Sounder measurements using NOAA-18. Journal of Geophysics Research 116, D10106, doi:10.1029/2010JD015412

Karl, T. R., Hassol, S. J., Miller, C. D. , Murray, W. L., 2006. Temperature trends in the lower atmosphere: Steps for understanding and reconciling differences. U.S. Climate Change Science Program: Synthesis and Assessment Product 1.1, 180 pp.

Masahiro Kazumori and Hidehiko Murata, 2012. Initial assessment of FY-3A microwave temperature sounder radiance data in JMA's global data assimilation system. CAS/JSC WGNE Res. Activ. Atmos. Oceanic Modell. (in press)

Li Q., 2001. Development of Chinese geostationary meteorological satellite, 2001. Spacecraft Recovery Remote Sensing **22**: 13–19.

Lu, Q., Bell, W., Bauer, P., Bormann, N., Peubey, Carole., 2011. Characterizing the FY-3A Microwave Temperature Sounder Using the ECMWF Model. Journal of Atmospheric and Oceanic Technology 28, 1373-1389.

Lu Q, Bell W, Bauer P, Bormann N, Peubey C. 2011. An evaluation of FY-3A satellite data for numerical weather prediction. Quarterly Journal of the Royal Meteorological Society. 137: 1298–1311. DOI:10.1002/qj.834

Meng Z. 2004. The Polar Orbit Meteorological Satellite in China. *Eng.Sci.* 6: 1–5.

Mo, T., 1996: Prelaunch calibration of the Advanced Microwave Sounding Unit-A for NOAA-K. IEEE Trans. Microwave Theory Tech., 44, 1460–1469.

Pailleux, J. 1985. Use of satellite data in the ECMWF analysis system. Pp.15-25. ECMWF Workshop on high resolution analysis, 24-26 June.

Peubey, C., Bell, W., Bauer, P., and Di Michele, S., 2011. A study on the spectral and radiometric specifications of a post-EPS microwave imaging mission. ECMWF Tech. Memo. 643.

Saunders, R., Matricardi, M., and Brunel, P., 1999. A fast radiative transfer model for assimilation of satellite radiance observations - RTTOV-5. ECMWF Tech. Memo. 282.

Zou, C.-Z., Goldberg, M. D., Cheng, Z., Grody, N. C., Sullivan, J. T., Cao, C., and Tarpley, D., 2006. Recalibration of Microwave Sounding Unit for climate studies using simultaneous nadir overpasses. J. Geophys. Res., 111, D19114, doi:10.1029/2005JD006798.

Zou, X., Wang, X., Weng, F., Li, G., 2011. Assessments of Chinese Fengyun Microwave Temperature Sounder (MWTS) Measurements for Weather and Climate Applications. Journal of Atmospheric and Oceanic Technology 28, 1206-1227.